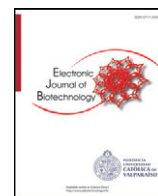




Contents lists available at ScienceDirect

Electronic Journal of Biotechnology



Research article

Molecular characterization of matrix metalloproteinase-1 (MMP-1) in *Lucilia sericata* larvae for potential therapeutic applicationsHamzeh Alipour^{a,b,1}, Abbasali Raz^{a,1}, Sedigheh Zakeri^a, Navid Dinparast Djadid^{a,*}^a Malaria and Vector Research Group, Biotechnology Research Center, Pasteur Institute of Iran, Tehran, Iran^b Department of Medical Entomology School of Health, Research Center for Health Sciences, Shiraz University of Medical Sciences, Shiraz, Iran

ARTICLE INFO

Article history:

Received 19 March 2017

Accepted 27 June 2017

Available online 1 July 2017

Keywords:

Alignment

Bioinformatics

Calliphoridae

Endopeptidase

Insects

Rapid Amplification of Genomic Ends

Rapid amplification cDNA ends

Regenerative medicine

Salivary glands

Three-dimensional structure

Wound healing

ABSTRACT

Background: The salivary glands of *Lucilia sericata* are the first organs to express specific endopeptidase enzymes. These enzymes play a central role in wound healing, and they have potential to be used therapeutically.**Methods:** Rapid amplification of cDNA ends and rapid amplification of genomic ends were used to identify the coding sequence of MMP-1 from *L. sericata*. Different segments of *MMP1* gene, namely the middle part, 3' end, and 5' end, were cloned, sequenced, and analyzed using bioinformatics tools to determine the distinct features of MMP-1 protein.**Results:** Assembling the different segments revealed that the complete mRNA sequence of MMP-1 is 1932 bp long. CDS is 1212 bp long and is responsible for the production of MMP-1 of 404 amino acid residues with a predicted molecular weight of 45.1 kDa. The middle part, 3' end, and 5' end sequences were 933, 503, and 496 bp. In addition, it was revealed that the *MMP-1* genomic sequence includes three exons and two introns. Furthermore, the three-dimensional structure of *L. sericata* MMP-1 protein was evaluated, and its alignment defined that it has high similarity to chain A of human MMP-2 with 100% confidence, 72% coverage, and 38% identity according to the SWISS-MODEL modeling analysis.**Conclusions:** MMP-1 of *L. sericata* has a close relationship with its homologs in invertebrates and other insects. The present study significantly contributes to understanding the function, classification, and evolution of the characterized MMP-1 from *L. sericata* and provides basic required information for the development of an effective medical bioproduct.© 2017 Pontificia Universidad Católica de Valparaíso. Production and hosting by Elsevier B.V. All rights reserved. This is an open access article under the CC BY-NC-ND license (<http://creativecommons.org/licenses/by-nc-nd/4.0/>).

1. Introduction

Matrix metalloproteinases (MMPs) are a family of endopeptidases that are prevalently known for their capability to break down the components of extracellular matrix (ECM) by degrading type I, II, and III native interstitial collagen [1]. A member of the MMP family, collagenase, was identified for the first time in 1962 [2]. Later, its primary structure, gene product, substrates, and therapeutic uses were reported and reviewed [3].

Lucilia sericata has been indicated to have a Holarctic distribution, but it can be found anywhere in the world, including in the Neotropical zones. There are also some reports of its distribution in Australia, Colombia, Argentina, Brazil, Chile, and Peru [3], as well as its presence in Iran [4,5]. *L. sericata* is considered a synanthropic species and has a close relation with human settlements and with a

necrophagous insect from the family Calliphoridae [6–8]. *L. sericata* has an important function in human medicine because it was the most common larval species used for maggot debridement therapy in ancient medicine for wound healing [9]. From the clinical point of view, two major effects of larval therapy have been ascribed: their secreted antibacterial compounds and their debriding mechanisms [10]. With regard to the latter function, it can be speculated that when the larvae spread out inside the wound, they secrete proteolytic enzymes that enable them to degrade and ingest necrotic tissues [11]. In addition, it has been revealed that 82 genes are expressed by *L. sericata* larvae at 4, 7, and 10 days during the regenerative process of wound healing [12]. Furthermore, transcriptome analysis revealed that one of the most important expressed transcripts is related to the matrix metalloproteinase family [12]. This species of flies, *L. sericata*, also plays a major role, as an agent of facultative myiasis, in humans and animals [13].

MMPs are a family of endopeptidases that are usually famous for their abilities to cleave the components of connective tissues in physiological and pathological processes [14]. MMPs have expanded

* Corresponding author.

E-mail address: navidmvr@gmail.com (N.D. Djadid).¹ These authors contributed equally to this work.

Peer review under responsibility of Pontificia Universidad Católica de Valparaíso.

physiological roles in biology for the regulation of cellular functions such as apoptosis, proliferation, differentiation, angiogenesis, migration, invasion, metastasis, and host defense [15]. Depending on their substrate specificities and sequence characteristics, MMPs are categorized into six main subclasses, namely collagenase, gelatinase, stromelysins, matrilysins, membrane-type MMPs, and others [16], which all are the main proteolytic enzymes responsible for food digestion in flies.

The ability to degrade different types of collagens (I, II, III, and IV) is the unique feature of MMPs. The proteolytic activity of MMPs can facilitate cell migration; produce specific substrate-cleavage fragments with independent biological activity; regulate tissue architecture through effects on the ECM and intracellular junctions; and activate, deactivate, or modify the activity of signaling molecules. Because cells have receptors for structural components of ECM, MMPs can also affect cellular functions by regulating the ECM proteins and their effects on cell interactions. In many cases, the cleavage of ECM substrates with MMPs generates fragments with different biological activities, compared to their precursors [17]. For instance, the cleavage of laminin-5 or collagen IV leads to the exposure of cryptic sites that promote cell migration. Degradation of type I collagen, which is mediated by *MMP-1*, is necessary for epithelial cell migration and wound healing in culture models [18]. The cleavage of ECM proteins by MMPs can also release ECM-bound growth factors, including insulin growth factors and fibroblast growth factors [19]. Recently, therapeutic methods are based on non-invasive approaches have been emphasized in medical society. In regenerative medicine, reducing the number of invasive procedures is the main objective, and it is the focal point of most related research studies. Collagenases catalyze the chemical processes and break the peptide bonds in collagen [20]. In some situations, collagen may be generated in more than the required amount, accumulate in unsuitable sites, or may not degrade after the specific time. In such cases, applying injectable collagenase or its ointment can be helpful in the degradation of the undesirable collagen deposits [21]. Furthermore, the therapeutic applications of collagenase have been demonstrated, both *in vitro* and *in vivo*, in different pathologic situations such as Peyronie's disease [22], glaucoma [23,24], wound healing [25], intervertebral disc herniation [26], burns [27], keloid [28], Dupuytren's disease [29], nipple pain [30], cellulite [31], and lipoma [32]. Concerning the importance of collagenase and its medical applications [33] and the fact that the only available collagenase with bacterial origin in the market has some side effects, this study was undertaken to identify and characterize collagenase-1 (*MMP-1*)- coding sequence (CDS) in *L. sericata* salivary gland transcriptome to provide basic information for future application-based studies.

2. Material and methods

2.1. Rearing of *L. sericata* larvae

Experiments were performed on the first instar of *L. sericata* maggots from a colony that had been reared in the facilities of NNHB Company established within the National Insectarium of Iran (NII), MVRG, Pasteur Institute of Iran (PII), under constant conditions. Adults were exposed to a 12-h light/dark cycle in a relative humidity of 40–50% at 18–25°C. The larvae were fed on ground chicken liver. Accurate species identification was routinely confirmed using morphological and molecular tools.

2.2. Primer design

Because the *L. sericata* genome has not been sequenced yet and on the basis of our previous study [34], rapid amplification of cDNA ends (RACE) and rapid amplification of genomic ends (RAGE) were selected for the determination of *L. sericata* collagenase sequence. First, the

mRNA sequences of MMPs from different insects such as *Musca domestica* (9XM_005179293.20), *Tribolium castaneum* (XM_008195377.1), *Culex quinquefasciatus* (XM_001861678.1), *Bombyx mori* (XM_004932241), and *Drosophila melanogaster* (NM_001259570.2) were aligned using the MEGA software (version 6.0). After analysis, four regions were chosen to design gene-specific primers (GSPs). LUF226, LUF293, LUF353, and LUF566 as well as R1138, R1205, R1289, and R1525 were designed as forward and reverse primers, respectively, to determine the middle part of the target gene. In the next step, on the basis of the middle part sequence of MMP1 mRNA molecule, GSPs were designed for 3' RACE (F1146, F1200, and F1359). The RAGE method was used to determine the 5' end sequence. GWA, GWB, GWC, GWD, GWE, GWF, GWG, UAP-N1, UAP-N2, LU5-243, LU5-317, LU5-377, and LU5-735 primers were used to perform RAGE in different reactions (Table 1).

2.3. Dissection of the salivary glands

The first instar maggots were anesthetized on ice and decapitated [35]. Dissection was performed in cold phosphate-buffered saline, pH 7.4 (150 mM NaCl and 10 mM Na₂HPO₄). The salivary glands were dissected 48 h post feeding on chicken liver. Six biological replicates, each consisting of salivary glands from three maggots, were collected for each time point and then kept at -70°C.

2.4. RNA extraction for standard reverse transcription-polymerase chain reactions

Total RNA was extracted from the salivary glands of the first instar of maggots using the total RNA purification kit (Jena Bioscience, Germany), and the extracted RNAs were treated by DNaseI (Fermentas, USA), both according to the manufacturer's instruction.

2.5. Reverse transcription (cDNA synthesis)

The single-stranded cDNA was synthesized using AccuPower RocketScript RT PreMix kit (Bioneer, Korea) following the

Table 1
List of the primers used in this study.

Experiments	Primer name	Sequence (5'–3')
Gene-specific primers	LUF226	AGCCGTGCAGGACTTTCAAAG
	LUF293	GAATTAATGTCAGTCCACGTTGTG
	LUF353	CGTTCTAAGCGTTATGCACTCCAG
	LUF566	GGTGATGGTGACGCTTTCGATG
	R1138	TGCCCTTGAAGAAATATGTTTTGCCA
	R1205	GTAAACCTTCACTAATCTCTTCGGGTA
	R1289	GCCAGAATTTACTGCCCTTATAGAAGTA
	R1525	TCTTGCAACCGAACCACAG
3' RACE	F1146	CATATTCTTCAAGGGCACAATATTG
	F1200	GTGATTACCCGAAGAGATTAGTGAAG
	F1359	CCAAACCGATTTCGAATTGGGAAG
5' genome walking	GWA	GATCAGGCGTCGCGTACCTCANNCTACTG
	GWB	GATCAGGCGTCGCGTACCTCANNCTACT
	GWC	GATCAGGCGTCGCGTACCTCANNCTACT
	GWD	GATCAGGCGTCGCGTACCTCANNACGGA
	GWE:	GATCAGGCGTCGCGTACCTCANNACCG
	GWF	GATCAGGCGTCGCGTACCTCANNACCG
	GWG	GATCAGGCGTCGCGTACCTCANNAGAC
	UAP-N1	CCTGTGAGCAGTCGTATCCACCAGTAC
		AGGCGTCGCGTACCTC
		CCTGTGAGCAGTCGTATCCAC
Full length	UAP-N2	TGAAAGTCCTGCACGGCTTTG
	Lu5-243	CACAACGTGGCAGTGACATTAATTC
	Lu5-317	CCTGGAGTGCATAACGCTTAGAAC
	Lu5-377	AAACCCAAAGAGTGACCAATTCATG
	Lu5-735	ATGGAATTAATGTCAGTCCAC
	Forward	CATTTCAGTAAGTATTTCTCTGATA
	Reverse	

manufacturer's instruction. Briefly, reverse transcription (RT) was performed in a final volume of 20 μ l by using random hexamer, linker, or GSP (according to the next reaction) as the primers. RT reaction was started with the following program: 10 min at 25°C, 60 min at 42°C, and 10 min at 70°C. All reagents were purchased from Fermentas (USA). Finally, genomic DNA contamination was checked using LUF226 and R1138 primers after the preparation of cDNA.

2.6. Polymerase chain reactions

All polymerase chain reactions (PCRs) were performed in a 20- μ l total volume for 35 cycles using 2 μ l of synthesized cDNA or 150 ng genomic DNA in each reaction as template. The reaction mixture contained 400 nM of each primer, 1.5 mM MgCl₂, 1 unit Taq DNA polymerase, 0.2 mM dNTPs, 2 μ l 10 \times reaction buffer, and 1.5 mM MgCl₂, and the final volume was adjusted to 20 μ l with double distilled water (DDW). The amplification program was set as follows: 5 min at 94°C; followed by 35 cycles of denaturation at 94°C for 30 s, annealing at 58°C for 30 s, and extension at 72°C for 80s; and an additional final extension at 72°C for 10 min.

The amplified amplicons were purified using the DNA gel purification kit (GF-1 Vivantis, Malaysia). The purified PCR products were adenine (A) and thymine (T) (complementary base pairs), which were TA-cloned into the pTG19-T vector (Vivantis, Malaysia) according to the manufacturer's instruction. Recombinant clones were selected using blue/white screening on Luria-Bertani agar plates containing X-gal (1.6 μ g/ml), IPTG (1.6 μ g/ml), and ampicillin (2 μ g/ml). White colonies were confirmed by colony PCR using universal (M13 forward and T7 promoter) and GSP primers. Four white colonies were picked for sequencing (Macrogen, Korea) in both directions.

2.7. Middle part mRNA sequence determination of the MMP-1

Salivary gland RNAs were extracted, and cDNA was synthesized using random hexamers, as described previously. To determine the middle part sequence, primers were designed according to the conserved regions of different MMP-1 mRNA sequences of five different insects, obtained from the NCBI (GenBank accession Nos: XM_005179293.2, XM_008195377.1, XM_001861678.1, NM_001123028.1, and NM_001259570.2; Tabel-1). Amplicons with size close to the predicted range were cloned into the pTG19-T vector. Plasmids were purified using the GeneJET Plasmid Miniprep Kit (Fermentas, Canada) and sequenced using M13 forward and reverse universal primers (Macrogen, Korea).

2.8. 3' RACE

On the basis of the middle part sequence of the *L. sericata* MMP-1 mRNA molecule, the sequence of which was determined in the previous step, three oligonucleotides were designed as GSPs. To perform 3' RACE reaction, first a linker was used to accomplish RT according to Raz et al.'s study [34] (Table 1). Then, the outermost GSP

(F1359) and outer primer were used as forward and reverse primers to performed the first PCR [34]. Then, the product of the first reaction was verified by internal GSPs (F1200, F1138, and F1146) and inner primer as forward and reverse primers, respectively [34]. After the confirmation, the first-round PCR product was TA-cloned, sequenced, and analyzed as before.

2.9. Determining the 5' end of *L. sericata* MMP-1 by RAGE

The RAGE method was used to determine the 5' end sequence of *L. sericata* MMP-1 DNA molecule. The schematic illustration is shown in Fig. 1. From the repeated sequences in different organisms, seven genome-walking primers (GWPs) were designed (Table 1). In the first step, single-stranded DNA (ssDNA) molecules were synthesized using the LU5-735 reverse primer in seven tubes from A to G separately. One tube was allotted for each GWP with a final volume of 15 μ l. Each tube contained 1.5 μ l PCR buffer 10 \times , 2 mM MgCl₂, 0.2 mM dNTPs, 400 nM GWP, 5 μ l cDNA, and 1 unit Taq DNA polymerase (Mix); the final volume was adjusted to 15 μ l with DDW. PCR was then set according to the following program: 5 min at 94°C for one cycle, followed by 25 cycles of denaturation at 94°C for 30 s, annealing at 59°C for 30 s, and extension at 72°C for 4 min. In the last cycle, the PCR product was further incubated at 72°C for 10 min. Then to confirm the ssDNA PCR products of each tube (A to G), these products were run on 1% agarose gel. In an ideal situation, no amplicon should be seen on the agarose gel. The second step was started without delay: 1.6 μ l GWP, 3.2 μ l Mix, and 1 unit of Taq DNA polymerase (5 U/ μ l) were added to each tube, which were labeled alphabetically from A to G. Then the PCR assay was performed according to Table 2. In the third step, PCR products of the previous step were diluted 1/25 (v/v), and 1 μ l of diluted product was used as template for this step with UAP-N1, Lu5-317, and Lu5-377 primers. PCR was performed with the following program: 5 min at 94°C for one cycle, followed by 35 cycles of denaturation at 94°C for 30 s, annealing at 58°C for 30 s, and extension at 72°C for 80 s. In the last cycle, the PCR product was further incubated at 72°C for 10 min. In the fourth step, the previous PCR products were diluted 1/25 and used as a template for PCR with Lu5-243 and UAP-N2 primers in seven separate reactions with the third-step PCR program. Finally, the PCR products of different GWPs were analyzed on 1.5% agarose gel, and sharp products were TA-cloned and sequenced.

2.10. Assembly of different fragments and total MMP-1 mRNA sequence determination

After identification of the middle and 3' and 5' end sequences of *L. sericata* collagenase, different fragments were assembled using the DNA Laser gene software (version 7.0). Finally, the assembled sequence was considered the full-length mRNA sequence of MMP-1 of *L. sericata*. This sequence was analyzed, its CDS was determined, and specific primers were designed to amplify the CDS and open reading frame (ORF) of MMP-1 gene for gene structure analysis. Full-length

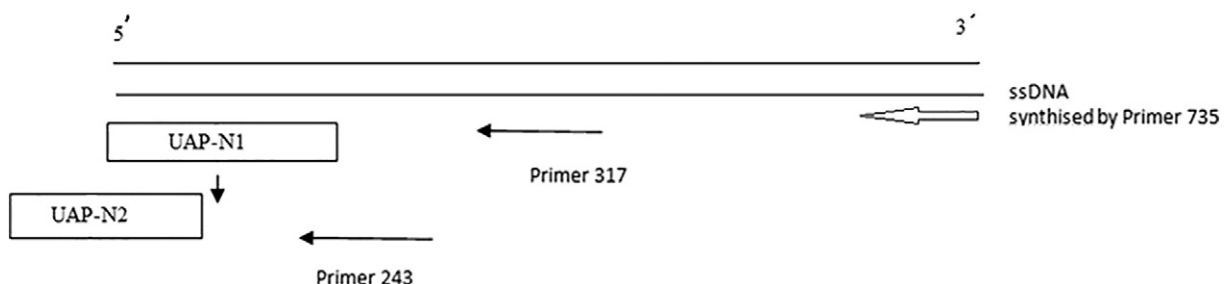


Fig. 1. Schematic illustration of the RAGE method to determine 5' ends.

Table 2
PCR program to recognize 5' ends in the RAGE method.

10 cycles from 2 to 3			7 cycles from 5 to 13										
94°C	34°C	72°C	72°C	94°C	15°C	72°C	94°C	65°C	72°C	94°C	36°C	72°C	72°C
4 min	1 min	1 min	5 min	30 s	30 s	3 min	30 s	30 s	30 s	30 s	60 s	3 min	15 min

molecular characterization was performed by the software mentioned in the “bioinformatics section”. The putative hemopexin and zinc-binding domains were determined with the NCBI BLASTp online tool.

2.11. Bioinformatics

All primers were designed using the GeneRunner software (version 4). Alignments were performed by the MEGA software (version 6.0), and their specificity for PCR was checked by nucleotide BLAST on NCBI (<http://blast.ncbi.nlm.nih.gov/Blast.cgi>). Moreover, ZincExplorer online software was used to predict zinc-binding sites according to its related protein sequence (<http://protein.cau.edu.cn/ZincExplorer>). Furthermore, Phyre2 web portal was used for the identification of similar proteins and determination of 3D structure.

To characterize the structural features of the protein coded by the assembled sequence and ensure that our sequence is a member of MMP-1 family enzymes, *L. sericata* MMP-1 was translated by GeneRunner software (version 4.0), and the deduced sequence was analyzed by different tools. First, protein BLAST was performed to determine proteins with high similarity to identify and score their characterization and classification. Similar proteins were selected to perform an alignment with Clustal Omega, based on the ClustalW method, to compare structural residues that are important for MMP protein classification. The presence of signal peptide was analyzed by SignalP 4.1 Server (<http://www.cbs.dtu.dk/services/SignalP/>), Signal BLAST (<http://sigpep.services.came.sbg.ac.at/signalblast.html>), and Signal-3L 2.0 online tools. The potential cleavage site to create the activated form of our target protein was predicted by PeptideCutter (http://web.expasy.org/peptide_cutter/) and PROSPER (<https://prosper.erc.monash.edu.au/webserver.html>), and its 3D structure was predicted by SWISS-MODEL (<https://swissmodel.expasy.org/>) and Phyre² (<http://www.sbg.bio.ic.ac.uk/phyre2/html/page.cgi?id=index>) servers.

The structural features of our target sequence was determined by comparing it with a similar protein, which had been determined by SWISS-MODEL and Phyre² servers with a high confidence score according to homology modeling. All alignments in this study were performed by the ClustalW method. Superimposition of the target protein with its fully characterized similar molecule and root-mean-square deviation (RMSD) calculation were performed using the DeepView/Swiss-pdbviewer (version 4.1.0) and UCSF Chimera (version 1.11.2) software.

3. Results and discussion

3.1. Characterization of the middle part of *L. sericata* MMP-1 mRNA and gene sequences

To determine the middle part sequence of *L. sericata* MMP-1 with different primer combinations, PCR reactions, which were performed using LUF226-R1205, LUF293-R1289, and LUF226-R1289 on the synthesized cDNA, showed amplification of amplicons near to the expected size of 979, 996, and 1063 bp, respectively (Fig. 2). Sequencing of these fragments and BLAST analysis revealed their high similarity (89%) with *M. domestica* MMP-14 mRNA sequence. The middle part sequence characterized in this step was submitted to GenBank (GenBank accession no: KP123435). *L. sericata* MMP-1

middle part mRNA sequence was aligned by Nucleotide BLAST, and it was revealed that the sequence showed 82% similarity to *M. domestica* MMP-14 mRNA sequence (XM_005179293). These steps were performed based on our previous studies on Carboxypeptidase B1 and Aminopeptidase N [34,36].

3.2. Characterization of the 3' end of *L. sericata* MMP-1 mRNA sequence

cDNA molecules synthesized by the linker primer were used as a template for primary PCR reactions with Outer as reverse and F1146, F1200, and F1350 as forward primers. The combination of Outer primer with all forward primers led to the amplification of amplicons with a favorable length. The amplicon related to F1200 Outer primer was confirmed using the inner primer as the reverse primer and by using F1200 and F1350 internal primers as forward primers. Therefore, the amplicon of the F1200 and Outer primer with 600-bp length (Fig. 3) was TA-cloned and sequenced, and its sequence was submitted to GenBank (GenBank accession no: KR996759). The RACE is a suitable method to detect 3' ends of unknown genes and only requires knowledge about the internal part of the target sequence [37,38].

3.3. 5' end of *L. sericata* MMP-1 mRNA sequence characterization

In the first step, ssDNA molecules were synthesized by Lu5-GSP, and different GWPs were then used for dsDNA production and their labeling. The other GSP (Lu5-377) in combination with UAP-N1 primer was used for the first nested PCR. The second nested PCR was carried out by combining third GSP (Lu5-317) with UAP-N2 (Fig. 4). Regarding the expected distance of 317 nucleotides from the 5' end of gene (600 bp), the PCR products with a size more than 600 bp were selected for recovery from the agarose gel, TA cloning and sequencing. Therefore, only GWC amplicon was selected for sequencing, and its

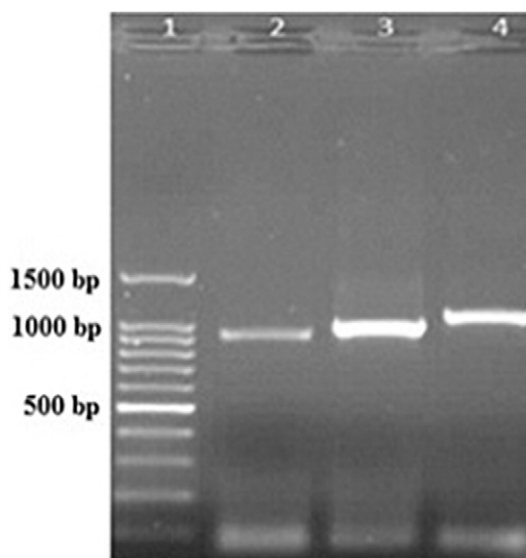


Fig. 2. Amplification of the middle part sequence of *L. sericata* MMP-1 mRNA. Different combinations of designed primers were evaluated to detect *L. sericata* MMP-1 middle part: Lane 1: Ladder 100 bp, Lane 2: LUF226-R1205 (979 bp), Lane 3: LUF293-R1289 (996 bp), and Lane 4: LUF226-R1289(1063 bp).

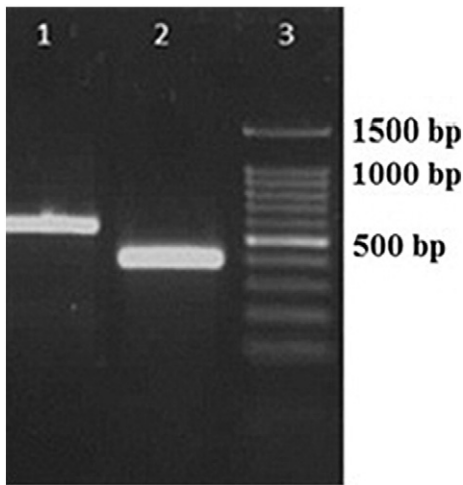


Fig. 3. 3' end characterization of the *L. sericata* MMP-1 mRNA sequence: After cDNA synthesis by a linker primer, F1200 and F1350 primers combined with inner primer were used for 3' end characterization of the *L. sericata* MMP-1 mRNA sequence. The amplicons of the F1200 and F1350 and the inner primer are indicated in lanes 1 and 2, respectively. Lane 3 is the 100-bp DNA marker.

analysis revealed that this amplicon is related to *L. sericata* MMP-1 gene sequence. The deduced sequence of 5' end of *L. sericata* MMP-1 mRNA was submitted to GenBank under accession no: KR996760. The RAGE method for DNA amplification by random fragmentation has been used by Makarov et al. [39].

3.4. Characterization of the *L. sericata* MMP-1 mRNA sequences

In accordance with our previous study, middle part, 3' end, and 5' end of the *L. sericata* MMP-1 mRNA sequence were identified stepwise [34]. These sequences were assembled by MEGA 7.0 software, and the total mRNA sequence of *L. sericata* MMP-1 was determined. On the basis of the assembled sequences, the CDS of *L. sericata* MMP-1 was determined and two specific primers were designed according to the start and stop codons to amplify the ORF and CDS of the target gene. We omitted the stop codon from the designed reverse primer. The synthesized cDNA with random hexamers and the extracted genomic DNA were used for the amplification of the CDS and ORF of *L. sericata* MMP-1. Our results revealed that the amplicons of the mRNA and DNA were 1212 bp (GenBank accession no: KY612612) and 1350 bp

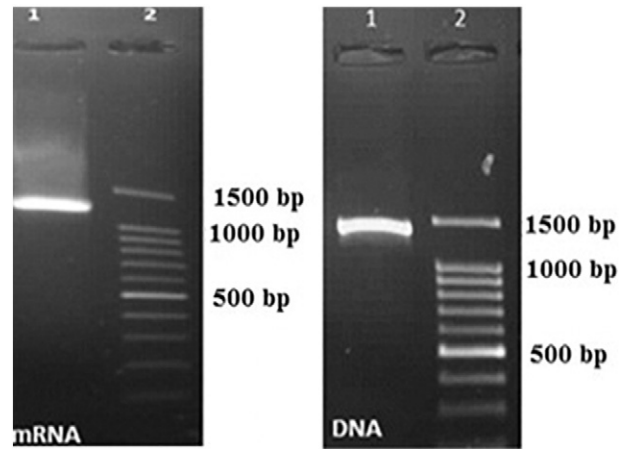


Fig. 5. PCR product of full-length DNA and mRNA of *L. sericata* MMP-1. 1) template 2) 100-bp marker.

(GenBank accession no: KY637052), respectively (Fig. 5). The alignment of the mRNA and DNA sequences of the MMP-1 demonstrated that its gene has two introns, wherein the length of the first and second introns is 68 bp and 65 bp, respectively.

3.5. Analysis of the cDNA and protein sequence of *L. sericata* MMP-1

The CDS of complete mRNA was started from nucleotides 494 to 1705. The comparison between mRNA and DNA sequences of *L. sericata* MMP-1 revealed that the whole genome of MMP-1 contains three exons and two introns. The first intron is located between nucleotides 257 and 325 and the second one between nucleotides 887 and 952.

L. sericata MMP-1 contains a 1212-bp ORF that encodes a protein of 404 amino acid residues with a predicted molecular mass of 45.1 kDa (Fig. 6). The CDS of *L. sericata* collagenase was TA-cloned in the pTG-19 vector and then sequenced, and its amino acid sequence was determined by GenRunner software. The BLAST result revealed that the protein sequence is very similar to the MMPs of insects and vertebrates, particularly MMP-2 in human and MMP-14 in *M. domestica* (Fig. 7). The comparison of our target protein sequence with similarly characterized related proteins identified a common catalytic domain, which is common in MMPs of different insects and some vertebrates (Fig. 5 and Fig. 6). Multiple predicted and hypothetical

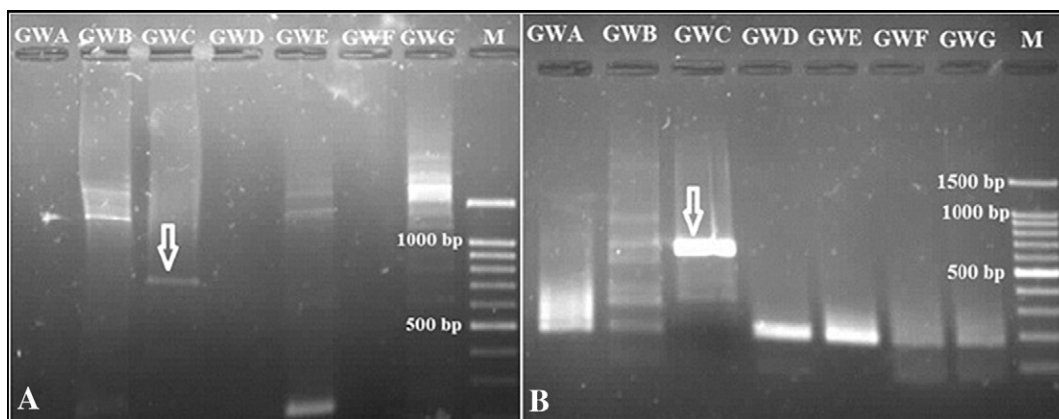


Fig. 4. 5' end of *L. sericata* MMP-1 mRNA sequence characterization: (A) First PCR reaction with the combination of LU5-377 and UAP-N1 primers on the product of GWA to G reactions from left to right, respectively. (B) The second PCR reaction on the product of LU5-377 and UAP-N1 primers with the combination of UAP-N2 and LU5-317. Only the amplicon of GWC was selected for further analysis. 100-bp DNA marker (CinaClon, Iran).

```

1 M E L M S L P R C G V R D K V G F
494 A T G G A A T T A A T G T C A C T G C C A C O T T O T O O T A C C C G A T A A G O T O G O C T T T
18 G N D N R S K R Y A L Q G S R W R
544 G O T A A T G A T A A T C O T T C C A A G C O T T A T G C A C T C C A G O O C A O C C O T T O O C O T
35 V K A L T Y K I S K Y P K R L K K
594 O T A A A G O C T T T O A C C T A T A A A A T C T C C A A A T A T C C T A A A C O T T T O A A G A A A
52 A D V D A E I A R A F A V W S E Y
644 O C T G A T O T T G A T O C C O A A A T T O C T A G A O C T T T T O C T O T C T O G A O C O A A T A C
69 T D L S F T P K S S G P V H I E I
694 A C C G A T C T A A G T T T T A C A C C C A A A A G T T C G G G A C C A G T A C A T A T T G A A A T T
86 K F V E S E H G D D D A F D G V G
744 A A A T T T G T T G A A A G T G A A C A T G O T G A T G O T G A C G C T T T C G A T G O T O T A G O T
103 G T T L A H A F F P V F G O D A H F
794 G G C A C T T T G C T C A T G C C T T C T T C C T G T C T T T G G T G G T G A T G C T C A T T T T
120 D D A E L W T I G S P R G T N L F
844 G A T G A T G C T G A A C T T T G G A C C A T T G C C A G T C C T C G T G C C A C T A A T C T T T T C
137 Q V A A H E F G H S L G L S H S D
894 C A A G T A G C T G C T C A T G A A T T T G G T C A C T C T T T G O O T T T G C A C A T T C C G A T
154 V R S A L M A P F Y R Q F E P V F
944 G T A C O T T C C G C T A A T G O C T C C C T T C T A T C O T G O T T T T G A G C C T O T T T T C
171 K L D S D D V L A I Q A L Y G K K
994 A A A T T G G A C T C T G A T G A T G T T T A G C C A T T C A G G C T T T A T A T G C A A G A A G
188 S S S N O N O I N P P S O O A F P
1044 T C C T C T C A A A T G G T A A T G G T A T A A T C C C C C C A G C G G T G G T G C C T T C C A
205 R T T Q R P A F A P R R T P R D D
1094 C G T A C C A C A A A G A C C C G C C T T T G C T C C A C C A C G C A C A C C C A G A G A T G A T
222 Q L C K D P K I D A L F N S A D G
1144 C A A T T A T O T A A A G A T C C C A A A A T T G A T O C T C T C T T C A A C T C A G C C O A T G O C
239 Q T Y A L K G N K Y Y K L T E N S
1194 C A G A C T T A T G C T C T T A A G G C C A A T A A A T A C T A T A A G C T T A C C G A A A A C T C A
256 V A D G Y P K L I S E G W P G L P
1244 G T G C C C G A C G G A T A T C C C A A A C T T A T C T C A G A A G G A T G G C C T G O T T T A C C A
273 O D I D A A F T Y K S O K T Y F F
1294 G O C G A T A T T G A T G C T G C T T T T A C C T A T A A A A O T G O C A A A A C A T A T T T C T T C
290 K G T K Y W R Y N G R Q M D G D Y
1344 A A G G O C A C C A A A T A T T O O C O T T A T A A T G O C C O T C A A A T O G A T O O T G A T T A C
307 P K E I S E G F T G V P D H L G A
1394 C C G A A A G A G A T T A G T G A A G O T T T A C T G G A G T G C C C G A T C A T T T G G A T G C T
324 A M V W G G N G K I Y F Y K G S K
1444 G C C A T G G T T T G G G C C G G T A A T G G T A A A A T T T A C T T C T A T A A G G G C A G T A A A
341 F W R F D P L K R P P V K S S Y P
1494 T T C T G G C G T T T C A T C C C T T G A A G A G A C C A C C A G T T A A G T C C A G C T A T C C C
358 F W R F D P L K R P P V K S S Y P
1544 T T C T O O C O T T T C A T C C C T T O A A G A G A C C A C C A G T T A A O T C C A O C T A T C C C
375 Q Y T N G Y T Y F F K G D K Y Y R
1594 C A A T A T A C C A A T G O T T A T A C G T A C T T C T T T A A G G O T G A T A A A T A C T A T C G G
392 F N D R T F A V S I S L I &
1644 T T T A A C G A T A G A A C A T T T G C A G T A A G T A T T T C T C T G A T A T G A

```

Fig. 6. Nucleotides and predicted amino acid sequence of *L. sericata* collagenase. Nucleotide and amino acid numbers are presented on the left. The amino acid sequence is shown as middle-letter code above the nucleotide sequence. The cysteine switch site is marked with box line 1 of protein sequence, and pro-peptide domain 1 (7–13 aa) containing the PRCGVRD conserved sequence is indicated in greyscale. The gray color region, known as the “active-site helix” encompasses part of the “zinc-binding consensus sequence”, VAAHEXXHXXGXXHS, which is the characteristic of the metzincin super family. The amino acids that are predicted to include in the active site and are involved in zinc binding are shown in boxes. Hemopexin-like repeats region (22–396AA) is shown by underline.

protein alignments from *L. sericata* MMP-1 and characterized insect MMPs showed highly conserved identity levels: 92% to MMP-14 from *Musca domestica* (GenBank: XM_005179293.2), 91% to MMP-14 from *Stomoxys calcitrans* (GenBank: XP_013100930.1), and 90% to MMP-14 isoform X1 from *Ceratitidis capitata* (GenBank: XP_004526293.1). Consequently, three repeats of fibronectin type-II domain inserted in the catalytic domain of *L. sericata* MMP-1 were identified. These findings indicate that *L. sericata* collagenase is an ortholog gene. Further sequence analysis identified a conserved pro-peptide domain with a cysteine-switch sequence (Fig. 6). There are a catalytic domain with conserved fibronectin repeats and a hemopexin-like (HPX) repeat domain with conserved metal-binding sites in the predicted

protein sequence (Fig. 6). MMPs have multiple domains, wherein one of these domains is HPX domain [40]. The comparison between the structure of the predicted *L. sericata* MMP-1 and fully characterized similar proteins of the vertebrates and insects demonstrated that *L. sericata* MMP-1 has all the structural features, which are typical for the members of these families (Fig. 6). In addition, *L. sericata* collagenase has PRCGVXD motif at positions 7–13, which is a conserved epitope in pro-domain of MMPs [41] (Fig. 6). This motif has an important role in enzyme latency [42]. This sequence maintains the latency of the secreted pro-enzyme through a ‘cysteine switch’ (Fig. 6). Domain 2 (138–152 aa) includes the active site and the catalytic ‘Zn’-binding region, VAAHEFGHSLGLSHS (Fig. 6). Some studies have revealed that

Species/Abbrv	
1. <i>L. sericata</i>	SPRGTNLFQVAAHEFGHSLGSLSHSDVRSALMAPFYRG-FEPVFKLSDDDLVAIQ
2. <i>M. domestica</i> XM_005179293.2 MMP14	SPRGTNLFQVAAHEFGHSLGSLSHSDVRSALMAPFYRG-YEPVFKLDTDDVLAIQ
3. <i>T. castaneum</i> XM_008195377.1 MMP1	SYRGTNLFQVAAHEFGHSLGSLSHSDVREALMAPFYRG-YDPLFELHEDDIQGIQ
4. <i>C. quinquefasciatus</i> XP_001861713 MMP1	KSRGTNLFQVAAHEFGHSLGSLSHSDVRSALMAPFYRG-YDPVFRLDSDVQGIQ
5. <i>B. mori</i> NP_001116499 MMP1	DEEGTSLFAVAVHEFGHSLGSLSHSSVKGALMYPWYQG-IQSNFVLPEDDRNGIQ
6. <i>D. melanogaster</i> NP_726473 MMP1	SPRGTNLFQVAAHEFGHSLGSLSHSDQSSALMAPFYRG-FEPVFKLDEDDKAAIQ
7. <i>Homo sapiens</i> NM_001304442 MMP8	TSANYNLFVAAHEFGHSLGSLSHSSDPGALMYPNYAFRETSNYSLPQDDIDGIQ
8. <i>Homo sapiens</i> NM_002427 MMP13	SSKGYNLFVAAHEFGHSLGSLSHSKDPGALMFPIYTYTGKSHFMLPDDVQGIQ
9. MMP2 homo sapiens EC:3.4.24.24	ATTANYDDDRKWFQCPDQCYSLFVAAHEFGHAMGLEHSDQDPGALMAPIYTY--TKNFRLSQDDIKGIQ
10. MMP9 Homo sapiens EC:3.4.24.35	ATTSNFDSDKKWGFQCPDQCYSLFVAAHEFGHALGLDHSVSPVPEALMYPMYRF--TEGPPHLKDDVNGIR
11. <i>C. histolyticum</i> D29981 colH	----IDKPLEEGNPDIIITMVIYNSPEEYKLSVLYGYDTNNGGMYIEPEGTFFTYEREAQESTYILE
12. <i>C. histolyticum</i> D87215 colG	----NDKALEVGNADDVLTMKIFNSPEEYKFNNTNNGVSTDNNGGLYIEPRGTFYTYERTPQQSIFSL

Fig. 7. Alignment of the substrate binding domain in zinc-peptidase MMP sequences of 12 organisms. Sequence comparison was performed using MEGA 6.0 software by the ClustalW method. The amino acids involved in zinc ion interaction and binding to the substrate are highlighted in yellow. "zinc-binding consensus sequence", VAAHEXXHXXGXXHS, is the characteristic sequence in the met-zinc super family.

the catalytic domain includes "HEXXHXXGXXH motif," which is the Zn²⁺ binding domain that supports the active site in MMP family members [43,44]. The position of hemopexin-like repeats is between 222 to 396 amino acids (Fig. 6). On the basis of these structural features, we propose that this nucleotide sequence codes another member of the MMP family. We also suggest the name *L. sericata* collagenase for this protein because it is the first MMP characterized in *L. sericata*, and its structure and sequence are very close to collagenase enzymes. In addition, it contains three His residues, which are involved in the coordination of the zinc atom at the active site and the Ser residue (Fig. 9). This interaction is the specific criterion that is

important in distinguishing the MMPs from other metalloproteinases. Furthermore, this catalytic domain has a Met residue [45].

3.6. Structural features of *L. sericata* collagenase

Amino acid composition of *L. sericata* collagenase is Ala (A) 7.9%, Arg (R) 5.2%, Asn (N) 3.7%, Asp (D) 7.7%, Cys (C) 0.5%, Gln (Q) 2.0%, Glu (E) 3.5%, Gly (G) 10.1%, His (H) 2.0%, Ile (I) 3.7%, Leu (L) 6.7%, Lys (K) 7.9%, Met (M) 1.2%, Phe (F) 6.9%, Pro (P) 6.7%, Ser (S) 7.7%, Thr (T) 4.5%, Trp (W) 2.0%, Tyr (Y) 5.7% and Val (V) 4.5%.

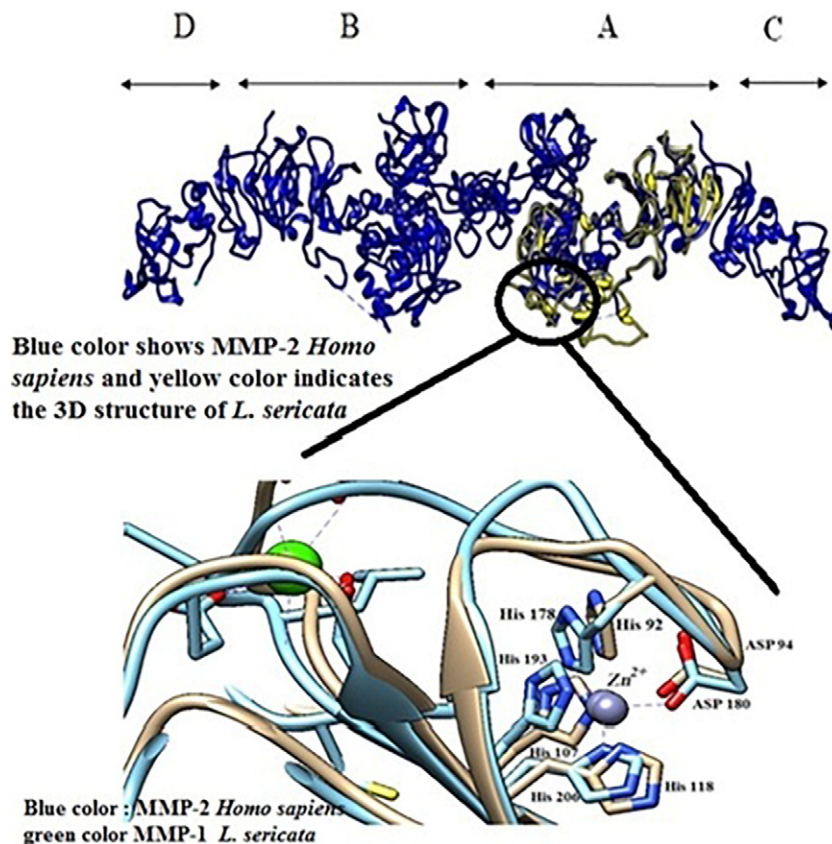


Fig. 8. Superimposition of 3D structure of chain A in MMP-2 human and MMP-1 *L. sericata*. 3D MMP-1 of *L. sericata* is similar to the chain A of human MMP-2. The structure of MMP-2 *Homo sapiens* containing four chains is shown (A–D).

Sequence analysis of the predicted protein suggests that it has metallo-endopeptidase activity and zinc-binding site. The zinc-binding sites were identified using Zinc Explorer software (<http://protein.cau.edu.cn/ZincExplorer/index.php?page=prediction>). The zinc-binding site of *MMP-1* was predicted to have Cys9, His92, Asp94, His141, His145, and His151 (Fig. 6). In addition, the 3D structure of *L. sericata* MMP-1 was predicted and analyzed with the Phyre2, and its results showed that the target sequence is similar to chain A of (72 kDa type IV collagenase) *MMP-2* of *Homo sapiens* with 100% confidence and 91% coverage, based on the PDB header. Human *MMP-2* has four chains, including A, B, C, and D, in its 3D structure (Fig. 8).

A phylogenetic tree of MMPs was constructed on the basis of the *MMP-1* protein sequence of different insects, humans, and *Clostridium histolyticum* by using the maximum likelihood method. Phylogenetic analysis showed that insect MMPs and bacterial collagenase are located in different phylogenetic groups as described by Kantor et al. [46]. Additionally, this result indicated that the highest similar physiological function and evolutionary relatedness were between the *M. domestica* MMP-14 and *L. sericata* (Fig. 9). In this approach, an initial tree is first constructed using a rapid but suboptimal method such as the neighbor-joining method, and its branch lengths are adjusted to maximize the likelihood of the data set for that tree topology under the desired model of evolution based on similar studies [47,48]. The phylogeny tree indicated a significant relationship between insect MMPs. In addition, human and insect MMPs considerably different from bacterial MMPs. Human *MMP-1* had a close relationship with insect *MMP-1*.

To qualify our target gene and its coded protein, its CDS was translated with GeneRunner software (version 4). A protein BLAST alignment was also performed for further comparison. At a glance, all the selected proteins were related to MMP enzyme family. Further comparison with PDB protein format revealed that our query is very similar to the chain; A: PDB molecule of *MMP-2* *Homo sapiens* (72 kDa type IV collagenase; accession no. EC:3.4.24.24) that was well characterized, and its 3D structure was released. Hence, *MMP-2* *Homo sapiens* with complete structural characteristics were selected as a model to determine the structural features of our target protein. This alignment revealed that the Cys9, His92, Asp94, His141, His145, and His151 positions are involved in the construction of the enzyme active site and they coordinate with the zinc ion, which acts as a co-factor, and they are necessary for enzyme activity (Fig. 8).

3.7. Three-dimensional structure prediction and superimposition

The 3D structure prediction was performed by SWISS-MODEL, which predicts the protein structures by homology modeling. According to the scores, the best matched result was related to human *MMP-2* (accession no: EC: 3.4.24.24). Hence, this model was selected for superimposition. The predicted 3D structure was illustrated by UCSF Chimera (Fig. 8). Our results revealed that *MMP-1* of *L. sericata* is similar to chain A of human *MMP-2*. Superimposition was performed by DeepView/Swiss-pdbviewer (version 4.1.0) and UCSF Chimera (version 1.11.2) software according to the previous study by Raz et al. [34] (Fig. 8). We compared the root-mean-square deviation (RMSD) of human *MMP-2* with our target protein for structurally important residues based on their carbon alpha atoms. In addition, the RMSD was performed to determine the residues in the most important domain among human *MMP-2* and *L. sericata* *MMP-1* (Table 3). Superimposition and RMSD calculation of human *MMP-1* and *L. sericata* matrix metalloproteinase were performed according to guidelines published by Koradi et al. [49].

3.8. Active site structure

In the active site of *MMP-1* *L. sericata*, the central zinc ion interacts with His 92, His 107, His 118, His 178, His 193, His 206, Asp 95, and Asp 180 (Fig. 8); thus, it seems that these residues are similar to those of human *MMP-2*. Superimposition of the active site between *MMP-1* *L. sericata* and *MMP-2* *Homo sapiens* revealed that six histidine residues are joint to each other (Fig. 7). Accordingly, the result of the current study is the first report of molecular characterization of *L. sericata* collagenase. Moreover, the comparison of 3D structure of *L. sericata* *MMP-1* and human collagenase (*MMP-2*) revealed that they have similar conformation, especially in zinc peptide and prodomain regions. Zinc binding is very important for proper and stable conformations of domains such that zinc finger proteins can function correctly [50]. The biological roles of zinc metal have been investigated, and it is shown that the exact prediction of zinc-binding sites is not only important for functional annotation of proteins but also helpful for 3D structure prediction [51,52]. All MMPs contain a signal peptide, a pro-peptide, and a Zn^{2+} -containing catalytic domain of 160–170 amino acids in length. Except for MMP-7, 23, and 26, all MMPs contain a proline-rich hinge region and a C-terminal

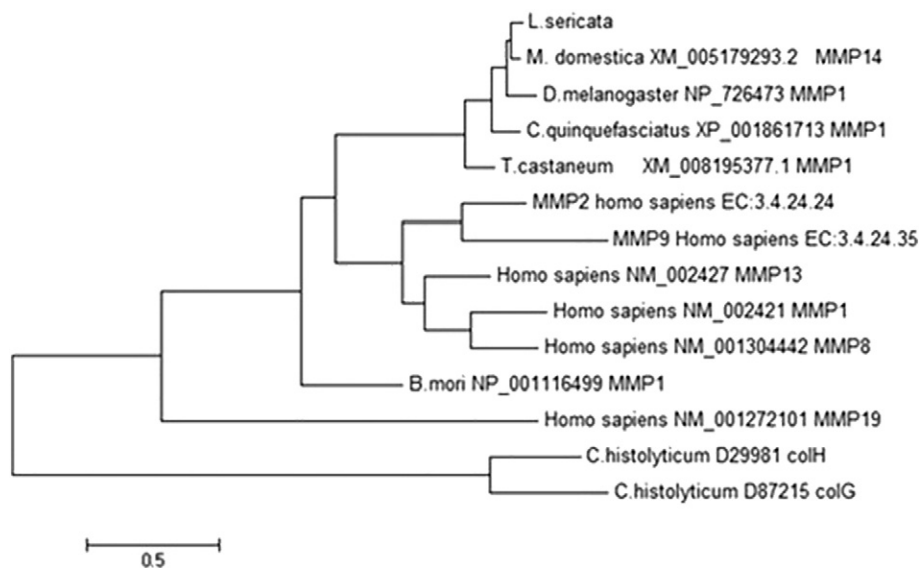


Fig. 9. Phylogenetic tree of MMPs. MMPs were aligned using MEGA 6.0 software based on the ClustalW method by using sequences characterized from insects, humans, and bacteria. The phylogenetic tree revealed that insect and human MMPs are genetically different from those of bacteria.

Table 3
The RMSD of residues in an important domain (active site).

Amino acid	HIS MMP-1	HIS MMP-1	HIS MMP-1	HIS Chain A	HIS Chain A	HIS Chain A	ASP MMP-1	ASP Chain A
Position	92	107	118	178	193	206	94	180
RMSD	1.49	2.83	2.64	2.11	2.21	3.32	1.74	2.53

hemopexin-like domain (PEX) [53]. Hemopexin is a heme-binding protein that transports heme to the liver [54]. Our results revealed that the hemopexin of *L. sericata* MMP-1 is located on amino acids 222 to 396. Following cleavage of distal to the highly conserved sequence (PRCGXPD) in the pro-peptide, latent MMPs (zymogen) become activated [55]. The alignment search revealed that the predicted amino acid sequence shares significant similarity with collagenase from various insects (Fig. 7). Phylogenetic analysis between *L. sericata* MMP-1 and human MMPs suggested they have a very close relationship with each other. This finding is similar to a previous result reported for *Tribolium castaneum* [56] that indicated its similarity with human MMP-2 (Fig. 9). The key feature of this enzyme is its ability to cleave interstitial collagens I, II, and III at a specific site at three-fourth distance from the N-terminus [57].

L. sericata maggots are used for the treatment of chronic wounds; this application is thought to be associated with the function of enzymes secreted by maggots [12,58]. In addition, it has been mentioned that the increment in the level of matrix metalloproteinase-9 is a consequence of events during the wound healing process [12]. The overexpression of MMP-2 during the extraction/secretion therapy indicates its involvement in accelerated repair of the wound healing process. Therefore, it is important to identify the coding sequence of these enzymes to provide basic information for their biomedical applications. As the collagenase enzyme plays an important role in wound healing, the present study has focused on determining the full-length CDS of *L. sericata* collagenase [59]. Maggot therapy can be used for cutaneous infection, but it is currently used for problematic wounds that are often poorly responsive to conventional drug treatments [60]. Our findings showed that *L. sericata* MMP-1 has striking structural similarities with MMP-2 of other organisms⁴⁵. These results strongly suggest that a conserved proteolytic system of tissue remodeling can be fully reconstituted in invertebrates. Because bacterial collagenases play an important role in pathogenesis, their practical applications in the treatment of diseases such as Dupuytren's contracture, liver cirrhosis, Peyronie's disease, wound healing, burns, cell isolation, and debridement have been considered safe, although they have some side effects [61,62]. Hence, to overcome these problems, it is required to screen novel sources of collagenase of non-pathogenic origin. Owing to the impressive effects of *L. sericata*-secreted enzymes in wound healing and the unique role of collagenase in this process and regenerative medicine, it is highly important to characterize a safe collagenase enzyme. This collagenase can be considered as an appropriate alternative because it is non-pathogenic. Therefore, the production of recombinant collagenase from non-pathogenic organism such as *L. sericata* was assessed by our team for its biomedical applications. By performing molecular characterization of the *L. sericata* CDS and its structural analysis, fundamental data were obtained for future studies to produce a safe and an effective agent for regenerative medicine.

This is the first report of full molecular characterization of an MMP-1 *L. sericata* gene from a medically important insect. In this study, we defined the CDS and ORF of the MMP-1 gene of *L. sericata*. The alignment of MMP-1 with ClustalW revealed that its structurally important residues are similar to well-characterized MMP-2 human enzymes. In fact, the residues of active sites (His 193, Asp 180, and His 92) are the same between the proteins of the present study and previously reported human MMP-2. Furthermore, after the modeling of MMP-1, superimposition with other different templates and overall RMSD value calculation revealed that the lowest score is related to

human MMP-2. These findings indicate that *L. sericata* MMP-1 has the nearest structure to human MMP-2 family as compared to different members of MMP family.

Financial support

The authors are grateful for the financial support provided by the educational office of Pasteur Institute of Iran (Grant No. TP-9124) to Hamzeh Alipour for his Ph.D. thesis and the Iranian National Science Foundation through grant 93011174 to NDD.

References

- Visse R, Nagase H. Matrix metalloproteinases and tissue inhibitors of metalloproteinases. *Circ Res* 2003;92(8):827–39. <http://dx.doi.org/10.1161/01.RES.0000070112.807113.D>.
- Gross J, Lapiere CM. Collagenolytic activity in amphibian tissues: A tissue culture assay. *Proc Natl Acad Sci* 1962;48(6):1014–22.
- Greenberg B. Nocturnal oviposition behavior of blow flies (*Diptera: Calliphoridae*). *J Med Entomol* 1990;27(5):807–10. <http://dx.doi.org/10.1093/jmedent/27.5.807>.
- Manouchehri A, Beesley W. The activity of sulphonamides against larvae of *Anopheles stephensi* (LISTON), *Aedes aegypti* (L.) and *Lucilia sericata* (MEIG.). *Mosq News* 1974;34(1):58–62.
- Rafinejad J, Akbarzadeh K, Rassi Y, Nozari J, Sedaghat MM, Hosseini M, et al. Traumatic myiasis agents in Iran with introducing of new dominant species, *Wohlfahrtia magnifica* (*Diptera: Sarcophagidae*). *Asian Pac J Trop Biomed* 2014;4(6):451–5. <http://dx.doi.org/10.12980/APJT.4.2014C1029>.
- Shiravi AH, Mostafavi R, Akbarzadeh K, Oshaghi MA temperature requirements of some common forensically important blow and flesh flies (*Diptera*) under laboratory conditions. *J Arthropod Borne Dis* 2011;5(1):54.
- Akbarzadeh K, Rafinejad J, Alipour H, Biglarian A. Human myiasis in Fars province, Iran. *Southeast Asian J Trop Med Public Health* 2012;43(5):1205.
- Alipour H, Raz A, Zakeri S, Dinparast Djadid N. Therapeutic applications of collagenase (metalloproteinases): A review. *Asian Pac J Trop Biomed* 2016;6(11):975–81. <http://dx.doi.org/10.1016/j.apjtb.2016.07.017>.
- Brundage AL, Crippen TL, Tomberlin JK. Methods for external disinfection of blow fly (*Diptera: Calliphoridae*) eggs prior to use in wound debridement therapy. *Wound Repair Regen* 2016;24(2):384–93. <http://dx.doi.org/10.1111/wrr.12408>.
- Cappelli L, Wigley FM. Management of Raynaud phenomenon and digital ulcers in scleroderma. *Rheum Dis Clin North Am* 2015;41(3):419–38. <http://dx.doi.org/10.1016/j.rdc.2015.04.005>.
- Pritchard DI, Čeřovský V, Nigam Y, Pickles SF, Cazander G, Nibbering PH, et al. TIME management by medicinal larvae. *Int Wound J* 2016;13(4):475–84. <http://dx.doi.org/10.1111/iwj.12457>.
- Polat E, İlayda Aksöz B, Arkan H, Coşkunpınar E, Akbaş F, Onaran I. Gene expression profiling of *Lucilia sericata* larvae extraction/secretion-treated skin wounds. *Gene* 2014;550(2):223–9. <http://dx.doi.org/10.1016/j.gene.2014.08.033>.
- Arabloo J, Grey S, Mobinizadeh M, Olyaeemanesh A, Hamouzadeh P, Khamisabadi K. Safety, effectiveness and economic aspects of maggot debridement therapy for wound healing. *Med J Islam Repub Iran* 2016;30:319.
- Hira PR, Assad R, Okasha G, Al-Ali FM, Iqbal J, Mutawali KEH, et al. Myiasis in Kuwait: Nosocomial infections caused by *Lucilia sericata* and *Megaselia scalaris*. *Am J Trop Med Hyg* 2004;70(4):386–9.
- McCarty SM, Cochrane CA, Clegg PD, Percival SL. The role of endogenous and exogenous enzymes in chronic wounds: A focus on the implications of aberrant levels of both host and bacterial proteases in wound healing. *Wound Repair Regen* 2012; 20(2):125–36. <http://dx.doi.org/10.1111/j.1524-475X.2012.00763.x>.
- Aielli G, Assiro R, Bacci C, Bartoli B, Bernardini P, Bi XJ, et al. Layout and performance of RPCs used in the Argo-YBJ experiment. *Nucl Inst Methods Phys Res Sect A* 2006; 562(1):92–6. <http://dx.doi.org/10.1016/j.nima.2006.02.136>.
- Duarte AS, Correia A, Esteves AC. Bacterial collagenases—A review. *Crit Rev Microbiol* 2016;42(1):106–26. <http://dx.doi.org/10.3109/1040841X.2014.904270>.
- Bonaventura P, Benedetti G, Albarède F, Miossec P. Zinc and its role in immunity and inflammation. *Autoimmun Rev* 2015;14(4):277–85. <http://dx.doi.org/10.1016/j.autrev.2014.11.008>.
- Rohani MG, Parks WC. Matrix remodeling by MMPs during wound repair. *Matrix Biol* 2015;44:113–21. <http://dx.doi.org/10.1016/j.matbio.2015.03.002>.
- Sawicka KM, Seeliger MS, Musaeu T, Macri LK, Clark RAF. *Adv Wound Care* 2015; 4(8):469–78. <http://dx.doi.org/10.1089/wound.2014.0616>.
- Stawikowski MJ, Stawikowska R, Fields GB. Collagenolytic matrix metalloproteinase activities toward peptomeric triple-helical substrates. *Biochemistry* 2015;54(19): 3110–21. <http://dx.doi.org/10.1021/acs.biochem.5b00110>.

- [22] Zhang Y-Z, Ran LY, Chun-Yang Li Chen XL. Diversity, structures, and collagen-degrading mechanisms of bacterial collagenolytic proteases. *Appl Environ Microbiol* 2015;81(18):6098–107. <http://dx.doi.org/10.1128/AEM.00883-15>.
- [23] Helin-Toivainen M, Ronkko S, Puustjärvi T, Rekonen P, Ollikainen M, Uusitalo H. Conjunctival matrix metalloproteinases and their inhibitors in glaucoma patients. *Acta Ophthalmol* 2015;93(2):165–71. <http://dx.doi.org/10.1111/aos.12550>.
- [24] Honig SC. Intralésional collagenase in the treatment of Peyronie's disease. *Ther Adv Urol* 2014;6(2):47–53. <http://dx.doi.org/10.1177/1756287213509849>.
- [25] Mathew SM, Ravisanker V, Potluri T, Suchithra T. Delayed diabetic wound healing: A focus on bacterial proteases in chronic wound and foot ulcer. *Int J Curr Res Rev* 2015; 7(12):36.
- [26] Zhang D, Zhang Y, Wang Z, Zhang X, Sheng M. Target radiofrequency combined with collagenase chemonucleolysis in the treatment of lumbar intervertebral disc herniation. *Int J Clin Exp Med* 2015;8(1):526.
- [27] Allen LM. Prior authorization of Santyl ointment (collagenase)—Pharmacy service; 2015.
- [28] Kang N, Sivakumar B, Sanders R, Nduka C, Gault D. Intra-lesional injections of collagenase are ineffective in the treatment of keloid and hypertrophic scars. *J Plast Reconstr Aesthet Surg* 2006;59(7):693–9. <http://dx.doi.org/10.1016/j.bjps.2005.11.022>.
- [29] Watt AJ, Curtin CM, Hentz VR. Collagenase injection as nonsurgical treatment of Dupuytren's disease: 8-year follow-up. *J Hand Surg* 2010;35(4):534–9. <http://dx.doi.org/10.1016/j.jhsa.2010.01.003>.
- [30] Kuşcu N, Koyuncu F, Lacin S. Collagenase treatment of sore nipples. *Int J Gynecol Obstet* 2002;76(1):81–2. [http://dx.doi.org/10.1016/S0020-7292\(01\)00550-1](http://dx.doi.org/10.1016/S0020-7292(01)00550-1).
- [31] Hexsel D, Orlandi C, Zechmeister D. Botanical extracts used in the treatment of cellulite. *Dermatol Surg* 2005;31(5):866–73. <http://dx.doi.org/10.1111/j.1524-4725.2005.31733>.
- [32] Matarasso A, Pfeifer TM. Mesotherapy for body contouring. *Plast Reconstr Surg* 2005;115(5):1420–4. <http://dx.doi.org/10.1097/01.PRS.0000162227.94032.ED>.
- [33] Alipour H, Raz A, Zakeri S, Dinparast Djadid N. Therapeutic applications of collagenase (metalloproteases): A review. *Asian Pac J Trop Biomed* 2016;6(11):975–81. <http://dx.doi.org/10.1016/j.apjtb.2016.07.017>.
- [34] Raz A, Djadid ND, Zakeri S. Molecular characterization of the carboxypeptidase B1 of *Anopheles stephensi* and its evaluation as a target for transmission-blocking vaccines. *Infect Immun* 2013;81(6):2206–16. <http://dx.doi.org/10.1128/IAI.01331-12>.
- [35] Telford G, Brown AP, Seabra RAM, Horobin AJ, Rich A, English JSC, et al. Degradation of eschar from venous leg ulcers using a recombinant chymotrypsin from *Lucilia sericata*. *Br J Dermatol* 2010;163(3):523–31. <http://dx.doi.org/10.1111/j.1365-2133.2010.09854.x>.
- [36] Bokharaei H, Raz A, Zakeri S, Dinparast Djadid N. 3'-RACE amplification of aminopeptidase N gene from *Anopheles stephensi* applicable in transmission blocking vaccines. *Avicenna J Med Biotechnol* 2012;4(3):131.
- [37] Frohman MA. 3'-end cDNA amplification using classic RACE. *Cold Spring Harb Protoc* 2006(1). [pdb. prot4130. <http://dx.doi.org/10.1101/pdb.prot4130>].
- [38] Autore F, Shanahan CM, Zhang Q. Identification and validation of putative Nesprin variants. *Nucl Envelope Methods Protoc* 2016;1411:211–20. http://dx.doi.org/10.1007/978-1-4939-3530-7_13.
- [39] Makarov VL, Sleptsova I, Kamberov E, Bruening E. DNA amplification and sequencing using DNA molecules generated by random fragmentation. 2016. Google Patents.
- [40] Cerofolini L, Amar S, Lauer JL, Martelli T, Fragai M, Luchinat C, et al. Bilayer membrane modulation of membrane type 1 matrix metalloproteinase (MT1-MMP) structure and proteolytic activity. *Sci Rep* 2016;6:29511. <http://dx.doi.org/10.1038/srep29511>.
- [41] Vishnuvardhan S, Ahsan R, Jackson K, Iwanicki R, Boe J, Haring J, et al. Identification of a novel metalloproteinase and its role in juvenile development of the tobacco hornworm, *Manduca sexta* (Linnaeus). *J Exp Zool B Mol Dev Evol* 2013;320(2):105–17. <http://dx.doi.org/10.1002/jez.b.22487>.
- [42] Seliger VI. Identification and evaluation of the predictive and diagnostic value of biomarkers applied to multi organ deficiencies in cystic fibrosis. Universität Ulm; 2014. <http://dx.doi.org/10.18725/OPARU-3014>.
- [43] Amor M, Moreno-Viedma V, Sarabi A, Grün NG, Itariu B, Leitner L, et al. Identification of matrix metalloproteinase-12 as a candidate molecule for prevention and treatment of cardiometabolic disease. *Mol Med* 2016;22:487. <http://dx.doi.org/10.2119/molmed.2016.00068>.
- [44] Benjami MM, Khalil RA. Matrix metalloproteinase inhibitors as investigative tools in the pathogenesis and management of vascular disease, in matrix metalloproteinase inhibitors. *Experientia Suppl* 2012;103:209–79. http://dx.doi.org/10.1007/978-3-0348-0364-9_7.
- [45] Chambers L, Woodrow S, Brown AP, Harris PD, Phillips D, Hall M, et al. Degradation of extracellular matrix components by defined proteinases from the greenbottle larva *Lucilia sericata* used for the clinical debridement of non-healing wounds. *Br J Dermatol* 2003;148(1):14–23. <http://dx.doi.org/10.1046/j.1365-2133.2003.04935.x>.
- [46] Kantor AM, Dong S, Held NL, Ishimwe E, Passarelli AL, Clem RJ, et al. Identification and initial characterization of matrix metalloproteinases in the yellow fever mosquito, *Aedes aegypti*. *Insect Mol Biol* 2017;26(1):113–26. <http://dx.doi.org/10.1111/imb.12275>.
- [47] Zhu X, Wang S, Shao M, Yan J, Liu F. The origin and evolution of Basigin (BSG) gene: A comparative genomic and phylogenetic analysis. *Dev Comp Immunol* 2017;72:79–88. <http://dx.doi.org/10.1016/j.dci.2017.02.007>.
- [48] Qu F, Xiang Z, Zhang Y, Li J, Xiao S, Zhang Y, et al. A novel p38 MAPK identified from *Crassostrea hongkongensis* and its involvement in host response to immune challenges. *Mol Immunol* 2016;79:113–24. <http://dx.doi.org/10.1016/j.molimm.2016.10.001>.
- [49] Koradi R, Billeter M, Wüthrich K. MOLMOL: A program for display and analysis of macromolecular structures. *J Mol Graph* 1996;14(1):51–5. [http://dx.doi.org/10.1016/0263-7855\(96\)00009-4](http://dx.doi.org/10.1016/0263-7855(96)00009-4).
- [50] Striedner Y, Schwarz T, Welte T, Futschik A, Rant U, Tiemann-Boege I. The long zinc finger domain of PRDM9 forms a highly stable and long-lived complex with its DNA recognition sequence. *Chromosome Res* 2017;1–18. <http://dx.doi.org/10.1007/s10577-017-9552-1>.
- [51] Golan Y, Itsumura N, Glaser F, Berman B, Kambe T, Assaraf YG. Molecular basis of transient neonatal zinc deficiency novel ZnT2 mutations disrupting zinc binding and permeation. *J Biol Chem* 2016;291(26):13546–59. <http://dx.doi.org/10.1074/jbc.M116.732693>.
- [52] Yao S, Flight RM, Rouchka EC, Moseley HNB. Perspectives and expectations in structural bioinformatics of metalloproteins. *Proteins Struct Funct Bioinf* 2017;85(5):938–44. <http://dx.doi.org/10.1002/prot.25263>.
- [53] Subramanian SR, Singam ERA, Berinski M, Subramanian V, Wade RC. Identification of an electrostatic ruler motif for sequence-specific binding of collagenase to collagen. *J Phys Chem B* 2016;120(33):8580–9. <http://dx.doi.org/10.1021/acs.jpcc.6b02573>.
- [54] Mitra A, Speer A, Lin K, Ehrst S, Niederweis M. PPE surface proteins are required for heme utilization by *Mycobacterium tuberculosis*. *MBio* 2017;8(1):e01720-16. <http://dx.doi.org/10.1128/mBio.01720-16>.
- [55] Kapoor C, Vaidya S, Wadhwan V, Hitesh, Kaur G, Pathak A. Seesaw of matrix metalloproteinases (MMPs). *J Cancer Res Ther* 2016;12(1):28–35. <http://dx.doi.org/10.4103/0973-1482.157337>.
- [56] Knorr E, Schmidtberg H, Vilcinskis A, Altincice B. MMPs regulate both development and immunity in the Tribolium model insect. *PLoS One* 2009;4(3):e4751. <http://dx.doi.org/10.1371/journal.pone.0004751>.
- [57] Shogan BD, Belogortseva N, Luong PM, Zaborin A, Lax S, Bethel C. Collagen degradation and MMP9 activation by *Enterococcus faecalis* contribute to intestinal anastomotic leak. *Sci Transl Med* 2015;7(286):286ra68. <http://dx.doi.org/10.1126/scitranslmed.3010658>.
- [58] Coskunpinar E, Arkan H, Dedeoglu BG, Aksoz I, Polat E, Araz T, et al. Determination of effective miRNAs in wound healing in an experimental rat model. *Cell Mol Biol* 2015;61(8):89–96. <http://dx.doi.org/10.14715/cmb.2015.61.8.15>.
- [59] Armstrong DG, Jude EB. The role of matrix metalloproteinases in wound healing. *J Am Podiatr Med Assoc* 2002;92(1):12–8. <http://dx.doi.org/10.1161/01.RES.0000070112.80711.3D>.
- [60] Gilead L, Mumcuoglu KY, Ingber A. The use of maggot debridement therapy in the treatment of chronic wounds in hospitalised and ambulatory patients. *J Wound Care* 2012;21(2):78. <http://dx.doi.org/10.12968/jowc.2012.21.2.78>.
- [61] Pearson JR, Zurita F, Tomás-Gallardo L, Díaz-Torres A, Díaz de la Loza MDC, Franze K, et al. ECM-regulator timp is required for stem cell niche organization and cyst production in the drosophila ovary. *PLoS Genet* 2016;12(1):e1005763. <http://dx.doi.org/10.1371/journal.pgen.1005763>.
- [62] Picardo NE, Khan WS. Advances in the understanding of the aetiology of Dupuytren's disease. *Surgeon* 2012;10(3):151–8. <http://dx.doi.org/10.1016/j.surge.2012.01.004>.